ICES Journal of
Marine Science

ICES Journal of Marine Science (2021), 78(4), 1444–1457. doi:10.1093/icesjms/fsaa255

Biogeographical patterns of meso- and bathypelagic fish along a Northeastern Atlantic transect

Eva García-Seoane*, Rupert Wienerroither, Kjell Arne Mork, Melanie J. Underwood, and Webjørn Melle

Institute of Marine Research (IMR), P. O. Box 1870 Nordnes, Bergen 5817, Norway

**Corresponding author: tel: +47 55 23 85 00; email:* eva.garcia.seoane@hi.no.

García-Seoane, E., Wienerroither, R., Mork, K. A., Underwood, M. J.and Melle, W. Biogeographical patterns of meso- and bathypelagic fish along a Northeastern Atlantic transect. – ICES Journal of Marine Science, 78: 1444–1457.

Received 3 July 2020; revised 14 December 2020; accepted 17 December 2020; advance access publication 13 March 2021.

The influence of oceanographic variables on assemblages of meso- and bathypelagic fish was investigated along a Northeastern Atlantic Ocean transect (Cape Verde to the Bay of Biscay) during May 2019. Fish were collected using a mrozooplankton trawl during daylight hours at ten stations. Along the transect, 17 hydrographic stations were also performed with a CTD (Conductivity, Temperature, and Depth). A total of 130 fish taxa were identified. The dominant family was Gonostomatidae, with four species (*Cyclothone braueri*, *Cyclothone microdon*, *Cyclothone pseudopallida*, and *Cyclothone pallida*) being responsible of more than 78% of the total density. The most frequent species that appeared to be ubiquitous were *C. braueri* and *C. pseudopallida*, while Myctophidae was the most diverse family. Multivariate analyses revealed two clusters related with the latitudinal gradient. The fish community in the southern stations (25–37°N) was more diverse than in the northern stations (42–48°N). Temperature from 300 to 700 m depth explained 65% of variation in terms of density and 58% in terms of biomass, both statistically significant. The investigated variation in the deep-pelagic ecosystems on a large spatial scale gives essential information to ecosystem management approhes and marine spatial planning.

Keywords: fish community, fish diversity, geographical distribution, micronekton, oceanography

Introduction

The deep-pelagic ocean (waters deeper than 200 m) is the largest habitat by volume on Earth (Webb *et al.*, 2010). In general, this dark environment is primarily cold and well oxygenated, but wide environmental variations do occur, for example in the oxygen minimum zones (OMZs) and the hydrothermal vent plumes (Thurber *et al.*, 2014). The conditions of the deep-sea have resulted in a specialized fauna, often dominated by species that are rare or absent in shallower waters, such as myctophids, stomiiforms, or mrourids (Drazen and Sutton, 2017). The deep-sea provides crucial ecosystem services, including the support of fisheries, the provision of energy, and mineral resources, as well as the regulation of the climate and nutrient cycling (Thurber *et al.*, 2014). Because of this and its vulnerability to threats such as overfishing and climate change (Webb *et al.*, 2010), it is necessary to increase our knowledge of the deep-pelagic ocean.

Fishes are an important component of the deep-sea ecosystems and, as intermediate trophic levels as well as top predators, a critical part of food webs (Drazen and Sutton, 2017). Both, the mesopelagic (water masses between 200 and 1000 m depth) and the bathypelagic zone (from 1000 m depth to ca. 100 m from the seafloor) belong to the deep-sea ecosystems (Sutton, 2013). Although the biomass of mesopelagic fish is still in question due to the uncertainty of the oustic estimations (Proud *et al.*, 2019), it probably dominates the global fish biomass (Irigoien *et al.*, 2014). The recent global estimates based on oustic methods ($\sim 10^{10}$ tons) are one order of magnitude larger than historical estimates based on net sampling (Gjøsæter and Kawaguchi, 1980; Irigoien *et al.*, 2014). Diel vertical migration, i.e. the tive

migration to the epipelagic zone (0–200 m depth) at night to feed, is a general feature of the species inhabiting the mesopelagic zone (Robinson *et al.*, 2010; Sutton, 2013). In this process, migrants tively transport carbon by respiration, excretion, and defecation to depth as well as being prey of carnivorous predators (Robinson *et al.*, 2010; Davison *et al.*, 2013). In addition, the efficiency of the energy transfer from phytoplankton to mesopelagic fish is higher than typically assumed, with mesopelagic fish respiring an estimated 10% of the primary production in deep waters (Irigoien *et al.*, 2014). Hence, due to their ubiquity, high biomass and that they may be respiring ~10% of the primary production in deep waters (Irigoien *et al.*, 2014), mesopelagic fish play an important role in the biological pump (Drazen and Sutton, 2017). Furthermore, trophic intertion of deep-pelagic fish and demersal fish on continental slopes bypassing the detrital flux and transferring carbon to deep long-term storage plays a key role in the ocean carbon cycle (Drazen and Sutton, 2017).

The Northeastern Atlantic is an interesting region to investigate meso- and bathypelagic fishes because of its varying geographic and oceanographic properties. The main ocean circulation pattern is the northern North Atlantic subpolar gyre (SPG) and the southern subtropical gyre (STG). The study area was mainly affected by the southern gyre, but in Bay of Biscay there was an intergyre zone with weak circulation, enclosed by the two gyres (Pollard *et al.*, 1996). This region is also influenced by the North Atlantic Drift, a northern branch of the Gulf Stream (Figure 1).

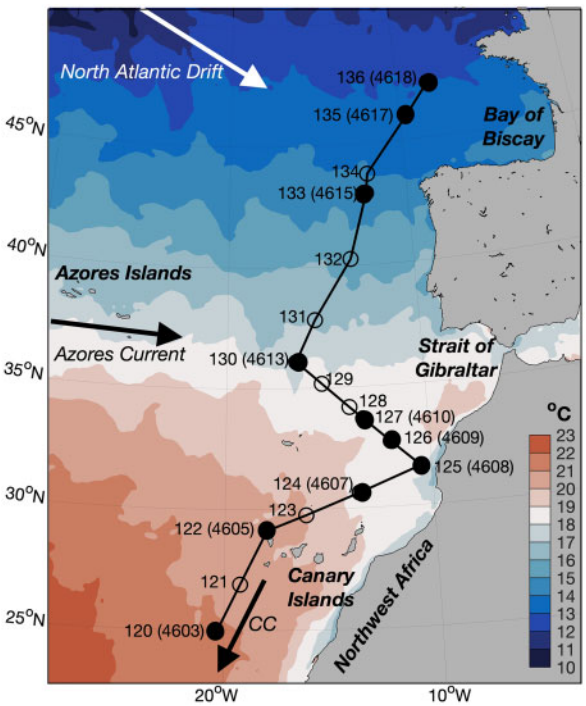

Figure 1. Map of the study area showing locations of the CTD stations (circles) and mroplankton trawls (filled circles), and with SST (°C) averaged over the period 2–22 May 2019. The CTD stations are numbered from 120 to 136, and the trawl stations (in parentheses) from 4603 to 4618. Only stations used in the analysis are numbered. Some currents, referred to in the text, are schematically included in the map. The SST data are daily means from satellite data and product of the operational Sea Surfe Temperature and Ice Analysis (OSTIA) system run by the UK Met Office (Donlon *et al.*, 2012).

The subtropical gyre (STG) is a wind-induced anticyclone gyre rehing down to 700–800 m depth in the eastern boundary (e.g. Valdés and Déniz-Gonzalez, 2015). It comprises of the eastward Azores Current in the north, which is a southern branch of the Gulf Stream, the southward Canary Current and the westward North Equatorial Current in the south at 15–20°N (e.g. Valdés and Déniz-Gonzalez, 2015; Figure 1). The northeasterly winds along the African coastline cause upwelling of colder water masses along the coast. The main water mass in the eastern STG is the North Atlantic Central Water (NW), which is the principal water mass in the upper layer of the North Atlantic (e.g. Bashmhnikov *et al.*, 2015). At intermediate levels, Mediterranean Overflow Waters (MOW) flow out through the Strait of Gibraltar and occupy the 700–1500 m depth. It is charterized by high salinities and temperatures (Carredo *et al.*, 2016) and low oxygen and nutrient contents (Bashmhnikov *et al.*, 2015). Northwest of the Iberian region below 500 m depth, NW gradually mixes with the MOW (Ríos *et al.*, 1992). Within this region, wind-induced upwelling events are common and the main source of primary production for most of the year (Tenore *et al.*, 1995).

Another principal water mass at intermediate level is Antarctic Intermediate Water (AAIW) that spreads northward from the Antarctic Circumpolar Current and along the African northwest coast to 30–32°N (Machín and Pelegrí, 2009). AAIW can be found at depth between 500 and 1200 m with a salinity minimum (Stramma and England, 1999). Originally, AAIW is oxygen rich, but the oxygen concentration decreases as it flows northward. In the central STG, high-salinity waters exist in the surfe layer (Subtropical Under Water), and near 20°N and 35°W, the salinity exceeds 37.0 psu, which is the highest in open ocean (O'Connor *et al.*, 2005).

There is a global pattern of mesopelagic fish species richness, with highest values in equatorial waters, followed by subtropical, temperate, and high-latitude waters (Backus *et al.*, 1977). The biomass of mesopelagic fish increases near large topographic structures like continental shelf breaks, seamounts, mid-ocean ridges, or volcanic islands (Hulley and Lutjeharms, 1989; Porteiro and Sutton, 2007; Sutton *et al.*, 2008; Wienerroither *et al.*, 2009). Recent studies on mesopelagic diversity in the northeastern central Atlantic (or in general) are mostly on a regional scale (e.g. Wienerroither *et al.* 2009; Ariza *et al.* 2016; García-Seoane *et al.* 2020), and variable sampling methods and gaps of information do not allow for statistical comparisons on a larger geographical scale. In spite of this limitation, Sutton *et al.* (2017) managed to present a global biogeographic classification of the mesopelagic zone reflecting regional variation of biodiversity and function. In our study, fish sampling covers two of these ecoregions: the North Atlantic drift region and the Central North Atlantic ecoregion. The North Atlantic drift ecoregion is a westerly wind biome, with large seasonal changes in mixed layer depth due to high westerly wind stress in winter (Sutton *et al.*, 2017). It is located in an intergyre zone enclosed by the STG and SPG (Pollard *et al.*, 1996), charterized by large spring algal blooms (Sutton *et al.*, 2017). The North Atlantic drift ecoregion is an eddy field area, expanding eastwards as the continuation of the Gulf Stream (Sutton *et al.*, 2017). On the other hand, the Central North Atlantic ecoregion is a trade wind biome with low productivity, weak seasonality, and a persistent deep maximum in chlorophyll (Sutton *et al.*, 2017). Small amplitude responses to trade with the variability of the wind are typical for this type of biome (Sutton *et al.*, 2017).

In terms of marine biodiversity, the deep-pelagic ocean is chronically underrepresented in the global databases (Webb *et al.*,

2010) and basic information on species composition, their distribution and the ftors that affect the community diversity is rare (Mengerink *et al.*, 2014). Considering the importance of deep-sea fish in the biological pump, knowledge of these species is needed for further investigations of the carbon flux. Hence, the aim of this work was to assess the influence of latitude and the oceanography on the meso- and bathypelagic fish assemblages along the Northeastern Atlantic Ocean.

Material and methods

Field sampling

A multidisciplinary cruise was conducted on board the *R.V.* "Kronprins Haakon" from 2 to 22 May 2019 along the eastern North Atlantic (from Cape Verde to northern France waters) (Figure 1). Meso- and bathypelagic fish were caught using a mrozooplankton trawl (Krafft *et al.*, 2010; Heino *et al.*, 2011) with a theoretical mouth opening of 6 × 6 m and a total length of 67 m. The gear consisted of a net of 8-mm stretched mesh and 3 × 3 mm light-opening from the start to the end. This prevented size-biased escapement from the trawl through differently sized mesh and avoided herding of organisms by larger meshes in the front. Hauls were conducted during daylight hours at ten stations. The net was towed obliquely at a speed around two knots, from the surfe to 1200 m depth, net geometry was recorded continuously. The sorting, subsampling, identification, and length and weight measurements were conducted on board. The total catch was weighed and, in case of a very high number of individuals, subsampled. Prior to subsampling, all large specimens were removed and the whole catch was checked for individuals of uncommon species (i.e. about 1 in 250 individuals). The subsample was randomly selected, weighed, and sorted. Subsample weights were obtained for eh taxon using a motion compensated balance, and these weights were extrapolated to the total catch by multiplying with the raising ftor (calculated by dividing the total catch by the subsample weight). For selecting the subsample size, we targeted having at least 100 individuals per species. Fishes were identified to the highest taxonomic category possible (Whitehead *et al.*, 1984–1986; Carpenter and De Angelis, 2016; Sutton *et al.*, 2020). Most specimens were identified to species, however, some small/juvenile or badly damaged specimens could only be identified to genus or family level. Length measurements were mainly to standard length, (some species were measured to total length following Mjanger *et al.* (2017)), and only undamaged specimens were measured. Validity of scientific names was checked with Fricke *et al.* (2020) and systematic order is cording to van der Laan *et al.* (2020).

Along the transect, 17 hydrographic stations were performed (Figure 1). At eh station, a Conductivity-Temperature-Depth (CTD) profiler cast was conducted down to 1200 m depth using a probe with an SBE 911plus CTD (Sea-Bird Electronics, WA, USA) and 12 water bottles rosette atthed. The CTD carried extra sensors for measuring dissolved oxygen concentration (SBE 43) and fluorescence (Wet Labs ECO-FL). The CTD-data were analysed and visualized with MATLAB software (MathWorks Inc.). At eh station, vertical averages were computed over 0–200, 300–700, and 700–1200 m depths, representing surfe, upper, and intermediate layers, for comparison with fish densities and biomasses.

Data analyses

Fish data were standardized using the filtered volumes (for density: individuals 10^3 m^{-3}; for biomass: g wet weight 10^3 m^{-3}) to compare the trawls. The volume of water filtered by the trawl was calculated using the vertical and horizontal opening of the trawl net as well as the trawl speed through water. The vertical opening was the distance between depth recorders pled on the headline and the footrope (Starmon TD; Star-Oddi, Gardabaer, Iceland), the horizontal opening was measured with oustic trawl instruments (SCANMAR AS, Åsgårdstand, Norway). A trawl-mounted oustic Doppler current profiler (ADCP; Signature500 in deep-water housing; Nortek AS, Rud, Norway) was used to measure the water flow in 50-cm bins ross the trawl's cross-section. The ADCP was mounted inside the trawl on the footrope and the water flow was averaged over all bins between the trawl netting to calculate the speed of the trawl through the water.

To calculate the sampled volume per minute, the average area of the opening of the trawl net was multiplied by the distance the trawl moved (60× speed of the trawl). Vessel propeller turbulence limited the use of the ADCP close to the vessel and therefore the sample volumes were calculated when the headline rehed 20 m. The sampled volumes per minute along a single trawl trk were then summed to estimate the total sampled volume of the haul.

Diversity was assessed based on Species Richness (S) calculated for eh haul. Taxa that are not typically meso- or bathypelagic but epipelagic or epibenthic were not excluded from the analyses because we cannot be sure where they were caught (surfe waters or below 200 m depth). The barplot graphs were constructed with R statistical software (R Development Core Team, 2019).

Patterns of the meso- and bathypelagic fish community structure were investigated using PRIMER 7 with PERMANOVA + (Anderson *et al.*, 2008; Clarke and Gorley, 2015). In these analyses, both density and biomass data were fourth root transformed before analysis to reduce the weighting of dominant species (Clarke *et al.*, 2014). Rare species (i.e. those representing <0.1% of density or <0.5% of biomass) were excluded from the multivariate analyses. Therefore, a total 38 of taxa were employed in the construction of the data matrix for density and 37 in the data matrix for biomass. Bray–Curtis similarities were calculated for eh pair of hauls to produce a similarity matrix. This matrix was classified by non-metric multidimensional scaling (nMDS) with the group average linking method and by cluster analyses. To investigate the latitudinal differences, the SIMPROF procedure (with a significance level of 1% and 9999 permutations) was used to identify significant groups of samples. The SIMPER procedure was applied to identify the key species.

Data exploration was conducted to identify outliers and collinearity following Zuur *et al.* (2010). One haul with one outlier in fluorescence was discarded from the analyses. The ten environmental variables were checked for collinearity: average temperature, average salinity, and average oxygen (from 0 to 200 m depth, from 300 to 700 m depth, and from 700 to 1200 depth) and average fluorescence in the upper 200 m (Supplementary Figure S1). Collinear variables were removed after inspection of correlation between variables and the variation inflation ftor (VIF > 3) (Zuur *et al.*, 2010). The variable temperature at 0–200 m depth was perfectly collinear with salinity at 0–200 m depth, and with average fluorescence at 0–200 m depth, as well as the temperature at 700–1200 m depth with the salinity at 700–1200 m depth. Thus, these two salinity variables were excluded before conducting VIF analyses. The distance-based linear models (DistLM) and distance-based redundancy analysis (dbRDA) (Legendre and Anderson, 1999; McArdle and Anderson, 2001) were used to study the relationship between the fish assemblages

and the environmental variables selected (temperature at 300–700 m, oxygen at 300–700 m, and oxygen at 700–1200 m, Supplementary Figure S2) and to build the multivariate statistical model. To rank the resulting models, the Akaike information criterion (AICc) was used, with the Step-wise selection criteria and 9999 permutations. AICc is a modification of the AIC and handles better situations where the ratio of samples to predictor variables is relatively small (Anderson *et al.*, 2008).

Results

Oceanography ross the North Atlantic

The sea surfe temperature (SST) along the cruise trk ranged from 21°C at the southernmost station to 12°C at the northernmost station in the Bay of Biscay (Figure 1). A lower SST (~18°C) along the northwestern coast of Africa, due to coastal upwelling of colder water masses, was clearly observed. The general trend along the transect northwards in the surfe layer (0–200 m) is a decline in both temperature and salinity and an increase in oxygen (Figure 2). From station 120 to 136, the temperature decreased by 8°C (i.e. from 20°C to 12°C). Highest salinity in the surfe layer (36.8 psu) was observed at station 120. The fluorescence in the surfe layer had a stable lower level south of 40°N (stations 120–131; 0.2 mg/m^3 or less). At stations 132–135, the fluorescence increased to 0.3–0.5 mg/m^3, and at the northernmost station 136, it was substantially higher (1.2 mg/m^3) compared to the other stations (Figure 2d). In the upper layer, 300–700 m depth, the temperature and salinity varied little along the transect while the oxygen varied most at this depth (3.3 ml/l at station 121 in the south to 5.4 ml/l at station 136 in the north). In the intermediate layer (700–1200 m depth), all three variables temperature, salinity, and oxygen increased with latitude. The plots of temperature and salinity show clearly that the northern part of the section had a weaker vertical stratification compared to the southern part. In the northern part, temperature and salinity showed little differences between the three layers (e.g. the temperatures varied between 10°C and 13°C at stations 133–136) indicating a nearly homogenous water column. This is in contrast to the southern part where the temperature and salinity decreased heavily with depth (e.g. from about 20°C in the upper layer to about 7°C at 700–1200 m depth at station 120).

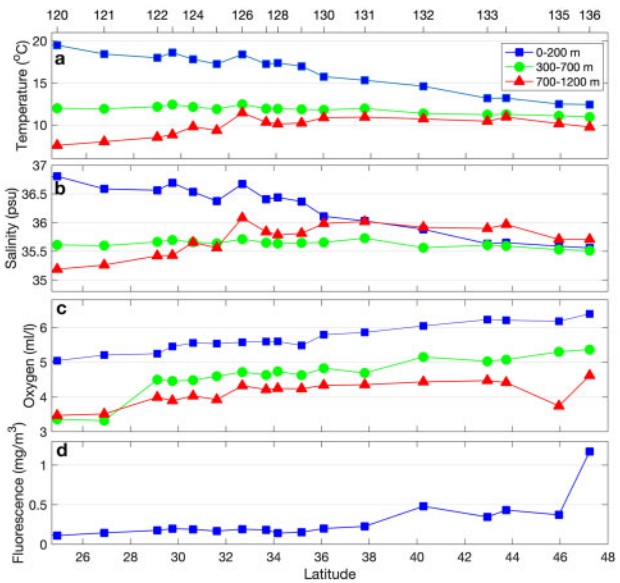

Figure 2. Average (a) temperature (°C), (b) salinity, (c) oxygen (ml/l) in three depth ranges (from 0 to 200, 300 to 700, and 700 to 1200 m), and (d) fluorescence (mg/m^3) from 0 to 200 m for eh CTD station.

Fish diversity and distribution ross the North Atlantic

A total of 18 orders and 36 families were recorded for at least 130 taxa (Table 1). The dominant family was Gonostomatidae. Four species of this family (*Cyclothone braueri*, *Cyclothone microdon*, *Cyclothone pseudopallida*, and *Cyclothone pallida*) were responsible for more than 78% of the total density. Due to the small size of *Cyclothone* spp., these four species together counted for only 28% to the biomass, with *C. microdon* dominating the biomass (almost 16% of the total biomass and *C. braueri* representing only 7%). Large growing specimens like *Eurypharynx pelecanoides* (ranging from 90–770 mm, Table 1), and *Serrivomer beanii* (ranging from 115 to 640 mm, Table 1), represent 12 and 5% of the biomass. The most species-rich family was Myctophidae (43 species) followed by the families Stomiidae (15) and Gonostomatidae (11). Among the myctophids, the most abundant species in terms of number were *Benthosema glaciale* and *Lobianchia dofleini*, while by weight they were *Lampanyctus cuprarius*, *B. glaciale*, and *Lampanyctus ater*. *Valenciennellus tripunctulatus*, *Argyropelecus hemigymnus*, and *Sternoptyx* spp. were the most numerous Sternoptychidae, whereas in terms of biomass the most important was *Maurolicus muelleri*. The most frequent species were *C. braueri* and *C. pseudopallida*, which appeared in all the hauls. *Cyclothone microdon*, *L. ater*, and *S. beanii* appeared in nine of the ten hauls analysed.

Several species, like *A. hemigymnus*, *C. braueri*, *C. microdon*, *C. pseudopallida*, *Notolychnus valdiviae*, and *S. beanii*, were caught at almost all stations, and thus appear to be ubiquitous (Supplementary Figure S3). Other species, such as *E. pelecanoides*, the myctophids *Benthosema suborbitale*, *Hygophum hygomii*, *Hygophum taaningi*, *L. dofleini*, *Notoscopelus resplendens*, the stomid *Chauliodus danae* and the sternoptychids *V. tripunctulatus* and *Sternoptyx* spp., showed a southern distribution from the coast of Africa to off the Cape S. Vicente, while the myctophid *B. glaciale* and the sternoptychid *M. muelleri* where only registered along the Galician coast and the Bay of Biscay (Supplementary Figure S3). Most of the species did not show a clear latitudinal size distribution (Supplementary Figure S4). However, *A. hemigymnus*, *C. pseudopallida*, *Diogenichthys atlanticus*, and *N. valdiviae* showed increasing sizes in northern and colder waters.

The highest species richness (63 taxa) was found at station 4610 (Figure 3a), which was off the coast of Morocco. The stations along the coast of Africa showed similar species richness, ranging from 48 to 63 taxa. However, the total number of taxa was considerably lower (between 17 and 20) in the northern stations (i.e. Bay of Biscay and off the coast of Galicia, northwestern Spain). Station 4607 showed low-density values (2.8 individuals/1000 m^3), which is particularly lower than at stations close-by (ranging from 7.1 to 13.1). The overall density from 0 to 1200 m depth ranged from 2.3 (in the Bay of Biscay) to 13.1 (the more coastal station) individuals/1000 m^3 (Figure 3b), whereas the biomass varied from 1.1 (in the Bay of Biscay) to 4.7 (north of the Canary Islands) g wet weight/1000 m^3 (Figure 3c). Both overall density and biomass were variable among stations, but lower biomasses were recorded from station 4613 northwards.

Table 1. Mean (number/1 000 m^3) and relative density (in % to the total community), mean (g weight/1 000 m^3), and relative biomass (in % to the total community), frequency of occurrence (%FO) and size range of the fish taxa caught at the ten stations (0–1 200 m) during May 2019.

			Density			Biomass				
Order	**Family**	**Species**	**Mean**	***SD***	**%**	**Mean**	***SD***	**%**	**FO**	**Range (mm)**
Anguilliformes	Derichthyidae	*Derichthys serpentinus*	0.0022	0.0038	<0.1	0.0140	0.0349	0.5	3	107–285
	Nemichthyidae	*Nemichthys curvirostris*	0.0005	0.0016	<0.1	0.0010	0.0031	<0.1	1	610
		Nemichthys scolopeus	0.0024	0.0063	<0.1	0.0090	0.0200	0.4	2	210–540
	Serrivomeridae	*Serrivomer beanii*	0.0199	0.0218	0.3	0.1328	0.1452	5.2	9	115–640
Scopharyngiformes	Eurypharyngidae	*Eurypharynx pelecanoides*	0.0289	0.0238	0.4	0.3164	0.3031	12.4	7	90–770
Alepocephaliformes	Alepocephalidae	*Asquamiceps* sp.	0.0005	0.0016	<0.1	0.0152	0.0480	0.6	1	138
		Conocara murrayi	0.0004	0.0012	<0.1	0.0003	0.0010	<0.1	1	46
		Einara sp.	0.0004	0.0012	<0.1	0.0221	0.0699	0.9	1	178
		Photostylus pycnopterus	0.0018	0.0033	<0.1	0.0062	0.0133	0.2	3	37–103
		Xenodermichthys copei	0.0079	0.0165	0.1	0.0168	0.0473	0.7	4	15–157
	Platytroctidae	*Barbantus curvifrons*	0.0013	0.0022	<0.1	0.0113	0.0264	0.4	3	56–112
		Maulisia mauli	0.0009	0.0019	<0.1	0.0005	0.0011	<0.1	2	42–43
		Mentodus spp.	0.0042	0.0060	<0.1	0.0011	0.0015	<0.1	6	19–51
		Normichthys operosus	0.0024	0.0033	<0.1	0.0334	0.0546	1.3	4	38–144
		Searsia koefoedi	0.0118	0.0121	0.2	0.0049	0.0041	0.2	8	18–71
Argentiniformes	Bathylagidae	*Bathylagus* spp.	0.0026	0.0069	<0.1	0.0015	0.0036	<0.1	2	31–50
		Melanolagus bericoides	0.0004	0.0013	<0.1	0.0004	0.0013	<0.1	1	24
	Opisthoproctidae	*Monoa grimaldii*	0.0004	0.0012	<0.1	0.0011	0.0033	<0.1	1	44
		Opisthoproctus soleatus	0.0011	0.0017	<0.1	0.0157	0.0292	0.6	3	56–90
Stomiiformes	Gonostomatidae	*Bonapartia pedaliota*	0.0167	0.0152	0.2	0.0150	0.0151	0.6	7	15–73
		Cyclothone braueri	2.5197	1.8222	35.8	0.1871	0.1151	7.3	10	10–36
		Cyclothone livida	0.0066	0.0140	<0.1	0.0009	0.0019	<0.1	2	24–33
		Cyclothone microdon	2.0924	1.8061	29.7	0.4069	0.2845	15.9	9	15–63
		Cyclothone pallida	0.3548	1.1221	5.0	0.0640	0.2023	2.5	1	22–58
		Cyclothone pseudopallida	0.5262	0.4914	7.5	0.0521	0.0373	2.0	10	16–42
		Diplophos taenia	0.0005	0.0016	<0.1	0.0029	0.0091	0.1	1	157
		Gonostoma denudatum	0.0011	0.0024	<0.1	0.0038	0.0100	0.1	2	51–117
		Margrethia obtusirostra	0.0044	0.0092	<0.1	0.0022	0.0042	<0.1	4	22–41
		Sigmops bathyphilus	0.0007	0.0022	<0.1	0.0001	0.0004	<0.1	1	33–36
		Sigmops elongatus	0.0111	0.0112	0.2	0.0334	0.0765	1.3	7	38–178
	Sternoptychidae	*Argyropelecus uleatus*	0.0228	0.0230	0.3	0.0295	0.0384	1.2	7	9–70
		Argyropelecus gigas	0.0044	0.0085	<0.1	0.0124	0.0251	0.5	3	11–83
		Argyropelecus hemigymnus	0.0960	0.0904	1.4	0.0175	0.0174	0.7	8	8–39
		Argyropelecus olfersii	0.0018	0.0056	<0.1	0.0001	0.0004	<0.1	1	10–15
		Maurolicus muelleri	0.0613	0.1688	0.9	0.0418	0.1107	1.6	3	11–52
		***Sternoptyx* spp.**	0.0876	0.1063	1.2	0.0235	0.0338	0.9	7	7–33
		Valenciennellus tripunctulatus	0.1522	0.1646	2.2	0.0223	0.0250	0.9	7	12–31
	Phosichthyidae	*Ichthyococcus ovatus*	0.0024	0.0034	<0.1	0.0008	0.0018	<0.1	4	14–37
		Vinciguerria attenuata	0.0108	0.0166	0.2	0.0036	0.0066	0.1	5	15–40
		Vinciguerria nimbaria	0.0063	0.0086	<0.1	0.0012	0.0026	<0.1	5	17–42
		Vinciguerria poweriae	0.0266	0.0217	0.4	0.0059	0.0048	0.2	7	17–37
	Stomiidae	*Astronesthes gemmifer*	0.0004	0.0011	<0.1	0.0003	0.0009	<0.1	1	45
		Astronesthes leucopogon	0.0004	0.0012	<0.1	0.0001	0.0002	<0.1	1	29
		Astronesthes micropogon	0.0004	0.0013	<0.1	0.0015	0.0047	<0.1	1	75
		Astronesthes niger	0.0005	0.0016	<0.1	0.0001	0.0003	<0.1	1	26
		Bathophilus pawneei	0.0004	0.0012	<0.1	0.0003	0.0008	<0.1	1	56
		Borostomias antarcticus	0.0004	0.0014	<0.1	0.0035	0.0111	0.1	1	110
		Chauliodus danae	0.0398	0.0330	0.6	0.0754	0.0643	3.0	7	27–133
		Chauliodus sloani	0.0152	0.0167	0.2	0.1333	0.1665	5.2	7	20–280
		Flagellostomias boureei	0.0004	0.0013	<0.1	0.0222	0.0703	0.9	1	303
		Idianthus fasciola	0.0033	0.0070	<0.1	0.0023	0.0043	<0.1	3	46–255
		Leptostomias spp.	0.0008	0.0016	<0.1	0.0003	0.0007	<0.1	2	57–64
		Malosteus niger	0.0018	0.0030	<0.1	0.0138	0.0245	0.5	3	74–182
		Photonectes braueri	0.0004	0.0013	<0.1	0.0209	0.0662	0.8	1	229
		Photostomias guernei	0.0104	0.0095	0.1	0.0245	0.0215	1.0	7	29–136
		Stomias boa boa	0.0025	0.0066	<0.1	0.0097	0.0258	0.4	2	62–180
Aulopiformes	Scopelarchidae	*Benthalbella infans*	0.0004	0.0011	<0.1	0.0005	0.0017	<0.1	1	78
		Scopelarchus analis	0.0055	0.0066	<0.1	0.0093	0.0115	0.4	5	40–73

Continued

Table 1. continued

Order	Family	Species	Density			Biomass			FO	Range
			Mean	*SD*	%	Mean	*SD*	%		(mm)
		Scopelarchus guentheri	0.0005	0.0016	<0.1	0.0006	0.0020	<0.1	1	55
	Paralepididae	*Paralepis brevirostris*	0.0057	0.0096	<0.1	0.0010	0.0017	<0.1	3	23–62
		Paralepis elongata	0.0029	0.0051	<0.1	0.0034	0.0085	0.1	3	36–95
	Evermannellidae	*Coccorella atlantica*	0.0004	0.0012	<0.1	0.0004	0.0012	<0.1	1	51
	Omosudidae	*Omosudis lowii*	0.0036	0.0061	<0.1	0.0052	0.0101	0.2	4	25–84
Myctophiformes	Myctophidae	***Benthosema glaciale***	0.2153	0.4594	3.1	0.0574	0.1230	2.2	3	12–44
		Benthosema suborbitale	0.0450	0.0624	0.6	0.0064	0.0088	0.2	6	12–31
		Bolinichthys indicus	0.0220	0.0186	0.3	0.0155	0.0136	0.6	7	26–47
		Bolinichthys supralateralis	0.0005	0.0016	<0.1	0.0002	0.0006	<0.1	1	31
		Ceratoscopelus warmingii	0.0054	0.0107	<0.1	0.0037	0.0061	0.1	4	18–54
		Dasyscopelus selenops	0.0025	0.0053	<0.1	0.0018	0.0039	<0.1	2	28–40
		Diaphus brhycephalus	0.0005	0.0016	<0.1	0.0008	0.0027	<0.1	1	43
		Diaphus holti	0.0013	0.0031	<0.1	0.0010	0.0021	<0.1	2	25–39
		Diaphus metopoclampus	0.0005	0.0015	<0.1	0.0003	0.0009	<0.1	1	32
		Diaphus mollis	0.0027	0.0058	<0.1	0.0038	0.0081	0.1	3	37–51
		Diaphus rafinesquii	0.0012	0.0025	<0.1	0.0027	0.0069	0.1	2	43–59
		Diogenichthys atlanticus	0.0350	0.0454	0.5	0.0035	0.0054	0.1	5	13–22
		Gonichthys cocco	0.0089	0.0152	0.1	0.0016	0.0032	<0.1	5	16–47
		Hygophum benoiti	0.0039	0.0074	<0.1	0.0010	0.0022	<0.1	3	12–48
		Hygophum hygomii	0.0443	0.0489	0.6	0.0153	0.0207	0.6	7	13–59
		Hygophum reinhardtii	0.0119	0.0142	0.2	0.0039	0.0050	0.2	6	13–47
		Hygophum taaningi	0.0462	0.0888	0.7	0.0245	0.0498	1.0	5	12–51
		Lampadena speculigera	0.0011	0.0025	<0.1	0.0004	0.0008	<0.1	2	28–35
		Lampadena urophaos atlantica	0.0005	0.0016	<0.1	0.0001	0.0005	<0.1	1	31
		Lampanyctus alatus	0.0183	0.0254	0.3	0.0200	0.0267	0.8	6	27–58
		Lampanyctus ater	0.0228	0.0189	0.3	0.0472	0.0465	1.9	9	25–119
		Lampanyctus crocodilus	0.0044	0.0072	<0.1	0.0371	0.0725	1.5	4	37–136
		Lampanyctus cuprarius	0.0596	0.1551	0.8	0.1151	0.3065	4.5	6	38–79
		Lampanyctus festivus	0.0004	0.0011	<0.1	0.0002	0.0006	<0.1	1	40
		Lampanyctus lineatus	0.0035	0.0068	<0.1	0.0249	0.0472	1.0	4	54–159
		Lampanyctus mdonaldi	0.0004	0.0014	<0.1	0.0005	0.0015	<0.1	1	54
		Lampanyctus photonotus	0.0029	0.0055	<0.1	0.0013	0.0021	<0.1	3	20–48
		Lampanyctus pusillus	0.0133	0.0193	0.2	0.0036	0.0060	0.1	5	21–47
		Lepidophanes gaussi	0.0106	0.0172	0.2	0.0052	0.0067	0.2	5	20–48
		Lepidophanes guentheri	0.0012	0.0027	<0.1	0.0023	0.0049	<0.1	2	43–64
		Lobianchia dofleini	0.0681	0.0780	1.0	0.0169	0.0199	0.7	7	14–36
		Lobianchia gemellarii	0.0052	0.0095	<0.1	0.0094	0.0142	0.4	4	20–63
		Myctophum punctatum	0.0209	0.0302	0.3	0.0067	0.0109	0.3	6	16–75
		Notolychnus valdiviae	0.0316	0.0319	0.4	0.0030	0.0032	0.1	8	13–25
		Notoscopelus bolini	0.0035	0.0057	<0.1	0.0012	0.0019	<0.1	4	24–39
		Notoscopelus caudispinosus	0.0004	0.0013	<0.1	0.0002	0.0008	<0.1	1	36
		Notoscopelus kroyeri	0.0137	0.0215	0.2	0.0038	0.0060	0.2	5	20–40
		Notoscopelus resplendens	0.0469	0.0960	0.7	0.0219	0.0431	0.9	6	23–48
		Protomyctophum arcticum	0.0004	0.0014	<0.1	0.0002	0.0007	<0.1	1	34
		Symbolophorus rufinus	0.0005	0.0016	<0.1	0.0045	0.0142	0.2	1	85
		Symbolophorus veranyi	0.0050	0.0086	<0.1	0.0015	0.0031	<0.1	3	22–43
		Taaningichthys bathyphilus	0.0023	0.0034	<0.1	0.0013	0.0018	<0.1	4	34–56
		Taaningichthys minimus	0.0008	0.0018	<0.1	0.0009	0.0022	<0.1	2	21–55
Lampriformes	Trhipteridae	indet.	0.0004	0.0012	<0.1	0.0008	0.0026	<0.1	1	178
Gadiformes	Bregmerotidae	*Bregmeros atlanticus*	0.0010	0.0031	<0.1	0.0006	0.0020	<0.1	1	33–55
	Melanonidae	*Melanonus zugmayeri*	0.0063	0.0143	<0.1	0.0017	0.0036	<0.1	3	25–47
	Gadidae	*Gadiculus argenteus*[a]	0.0004	0.0014	<0.1	0.0002	0.0006	<0.1	1	31
Beryciformes	Melamphaidae	*Melamphaes* spp.	0.0185	0.0180	0.3	0.0190	0.0189	0.7	7	15–71
		Poromitra capito	0.0017	0.0036	<0.1	0.0161	0.0371	0.6	2	64–91
		Poromitra crassiceps	0.0030	0.0081	<0.1	0.0299	0.0638	1.2	2	61–119
		Scopelogadus beanii	0.0004	0.0014	<0.1	0.0044	0.0138	0.2	1	75
		Scopelogadus mizolepis	0.0005	0.0015	<0.1	0.0017	0.0055	<0.1	1	59
	Rondeletiidae	*Rondeletia loricata*	0.0017	0.0029	<0.1	0.0177	0.0341	0.7	3	50–89
Trhichthyiformes	Diretmidae	*Diretmus argenteus*	0.0017	0.0023	<0.1	0.0231	0.0361	0.9	4	31–82
Ophidiiformes	Bythitidae	*Leucobrotula adipata*	0.0013	0.0042	<0.1	0.0003	0.0010	<0.1	1	34–50

Continued

Table 1. continued

Order	Family	Species	Density			Biomass			FO	Range (mm)
			Mean	*SD*	%	Mean	*SD*	%		
Scombriformes	Nomeidae	*Cubiceps grilis*	0.0004	0.0012	<0.1	0.0019	0.0060	<0.1	1	66
	Chiasmodontidae	*Chiasmodon niger*	0.0008	0.0018	<0.1	0.0071	0.0208	0.3	2	54–102
		Pseudoscopelus sp.	0.0004	0.0012	<0.1	0.0032	0.0102	0.1	1	90
	Scombridae	*Scomber colias*[a]	0.0007	0.0023	<0.1	0.0037	0.0117	0.1	1	85–95
	Gempylidae	*Diplospinus multistriatus*	0.0005	0.0016	<0.1	0.0002	0.0005	<0.1	1	80
Carangiformes	Carangidae	*Trhurus picturatus*[a]	0.0062	0.0185	<0.1	0.0518	0.1559	2.0	2	80–125
anthuriformes	Caproidae	*Capros aper*	0.0068	0.0110	<0.1	0.0078	0.0138	0.3	4	20–39
Lophiiformes	Melanocetidae	*Melanocetus* spp.	0.0014	0.0033	<0.1	0.0029	0.0064	0.1	2	19–23
	Diceratiidae	*Diceratias pileatus*	0.0005	0.0015	<0.1	0.0225	0.0711	0.9	1	89
ropomatiformes	Epigonidae	*Epigonus telescopus*[a]	0.0005	0.0016	<0.1	0.0000	0.0001	<0.1	1	17
	Howellidae	*Howella* spp.	0.0020	0.0037	<0.1	0.0050	0.0081	0.2	3	24–61
Perciformes	Callionymidae	indet.[a]	0.0004	0.0011	<0.1	0.0000	0.0001	<0.1	2	12–16
		Total	7.0351	7.6103		2.5536	3.763658			

SD indicates the standard deviation. Top 18 taxa regarding mean density are highlighted in bold and top 18 regarding mean biomass are highlighted in blue.
[a]Taxa epipelagic or epibenthic.

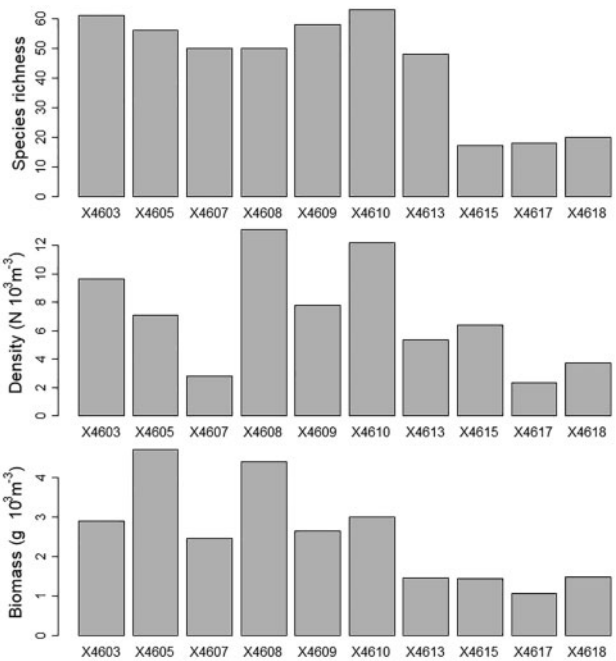

Figure 3. (a) Species richness (i.e. number of taxa), (b) overall fish density, and (c) overall fish biomass per station.

Fish community structure

The nMDS plots (both density and biomass) reveal two clusters related to the latitudinal gradient (Figure 5). Samples are more scattered in the density nMDS and more clustered in the biomass nMDS plot. In terms of density, the most scattered stations in the southern group were the most tropical (4603) and the more inshore station (4608) (in the right and left side of the group, respectively). Stress values were low for both nMDS ($\leq$0.01), being useful two-dimensional ordinations, with no prospect of misinterpretation (Clarke *et al.*, 2014).

Cluster analyses (using SIMPROF) separated the samples into two clusters in terms of density (Figure 6a), as well as in terms of biomass (Figure 6b). Again, all these clusters followed the north progression of the stations in the transect, confirming the clusters of the nMDS. In terms of density, there were no significant differences between stations from cluster 1 and the most different station was the most tropical station (4603). The most inshore station (4608) was also separate from the other southern stations. However, in terms of biomass, 4603 and 4605 are similar, and 4607 and 4608 as well.

The size of the individuals collected in the mrozooplankton trawl ranged between ten (*Argyropelecus olfersii*) and 770 mm (*E. pelecanoides*) (Table 1). No difference with respect to size range or modal size classes was evident between northern and southern areas for C. *braueri* and *C. microdon*. In contrast, some differences were found between north and south areas for *C. pseudopallida*, with bimodal distributions, but larger individuals being detected in the north (Figure 4). Densities and biomass per area for all taxa are given in detail in Supplementary Table S1.

The SIMPER routine identified the principal species in eh cluster regarding the taxa contribution to the average of similarity of eh cluster. In terms of density, the key species in cluster 1 (stations between 25–37°N) were *C. braueri*, *C. pseudopallida*, and *C. microdon* (counting for 22%) with other species such as *V. tripunctulatus*, *A. hemigymnus*, *Sternoptyx* spp., and *C. danae* contributing another 13% (Table 2). In cluster 2 (stations from 42–48°N), the rank was different, the key species being *C. microdon* (counting for 26%), *B. glaciale*, *C. braueri*, and *C. pseudopallida*, contributing another 48%. In terms of biomass, the key species were *E. pelecanoides*, *C. braueri*, and *C. danae* in cluster 1 (counting for 21% of the average similarity), while *C. microdon*, *B. glaciale*, and *Lampanyctus crocodilus* were key in cluster 2 (Table 3). Though the southern cluster 1 showed a higher number of charteristic taxa for both density and biomass data, the taxa contributed less to the similarity. The northern cluster 2 had less taxa, but they contributed more. However, cluster 2 included some species only charteristic of that cluster, such as *B. glaciale*, *M. muelleri*, and *Xenodermichthys copei*.

The relationship between meso- and bathypelagic fish community and environmental parameters

The DistLM marginal test showed that only temperature from 300 to 700 m depth was statistically significant ($p < 0.05$) and it

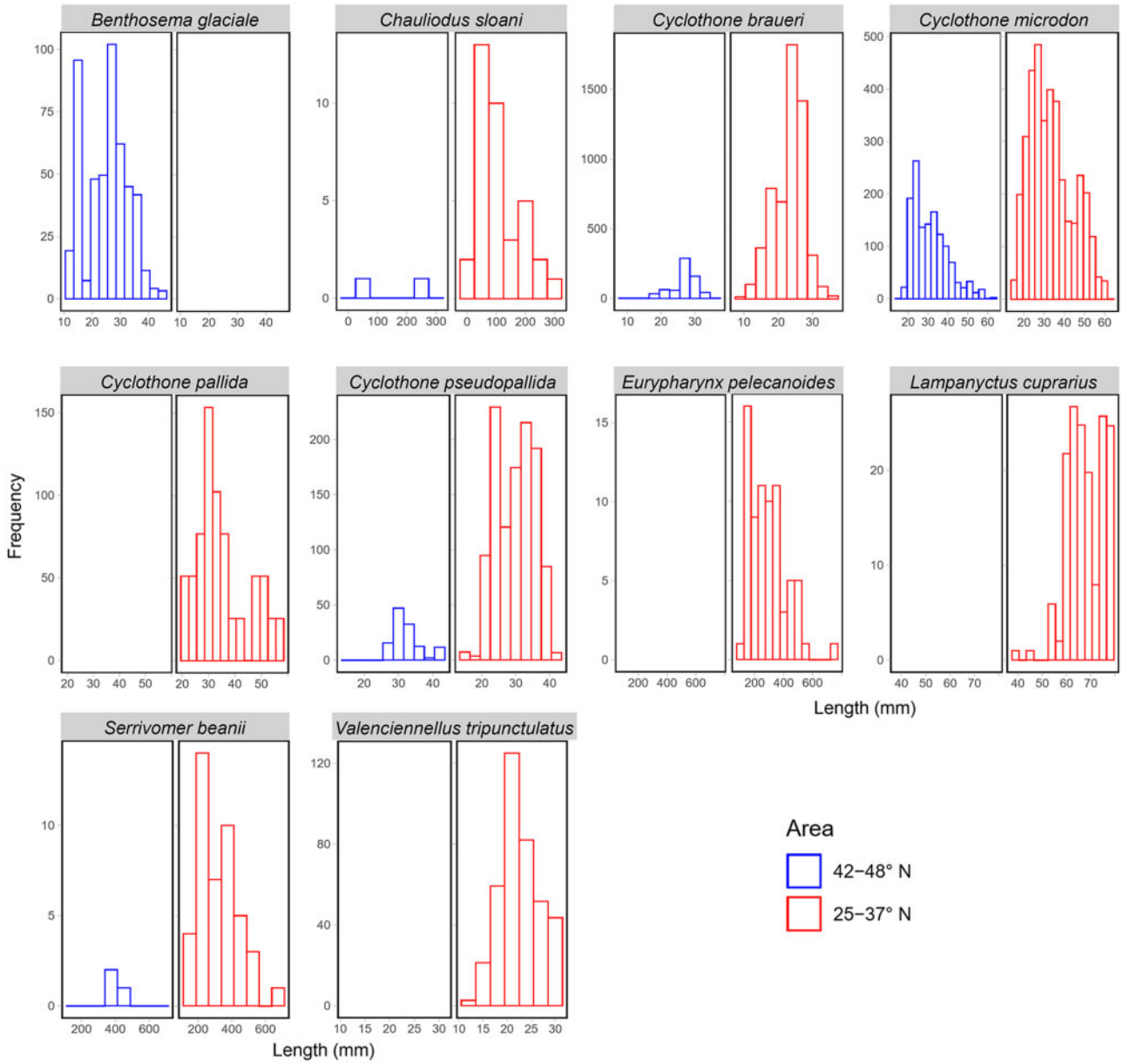

Figure 4. Length frequency distribution for the most abundant species collected in the different areas. Individuals were measured to standard length, except *E. pelecanoides* and *S. beanii* (which were measured to total length).

explained 65% of variation in terms of density (Table 4) and 58% in terms of biomass (Table 5). Oxygen at 300 to 700 m explained 39 and 35% in terms of density and biomass, but it is not significant. The model with smaller AICc values included only one variable (the temperature at 300–700 m depth) for both density and biomass data.

For both density and biomass data, the dbRDA showed similar patterns (Figure 7). There was discrimination among the latitudes, with the southern stations (25–37°N) associated with higher mean temperatures at 300–700 m and northern stations (42–48°N) associated with lower mean temperatures. The dispersion along the dbRDA2 axis 2, which is related to oxygen at 700–1200 depth, was present in both clusters and larger in terms of density than in biomass.

Discussion

Fish communities ross the transect

We have identified 42 of the 80 myctophid species reported in the Northeast Atlantic, 11 of the 18 gonostomatid species, and 15 species of the 108 stomiid species reported for the same area (Badcock, 1984; Gibbs, 1984; Hulley, 1984; Sutton *et al.*, 2020). Several studies (Sutton *et al.*, 2010; Olivar *et al.*, 2017) have also reported Myctophidae as the most speciose family of meso- and bathypelagic fish, followed by Stomiidae and Gonostomatidae, pointing to a general pattern in the North Atlantic Ocean. The gonostomatid fishes *C. braueri*, *C. microdon*, *C. pseudopallida*, and *C. pallida* dominate our samples despite midwater fish trawls not being optimal for the sampling of these smaller sized individuals (Gartner *et al.*, 1989; Olivar *et al.*, 2017). *Cyclothone* spp. are

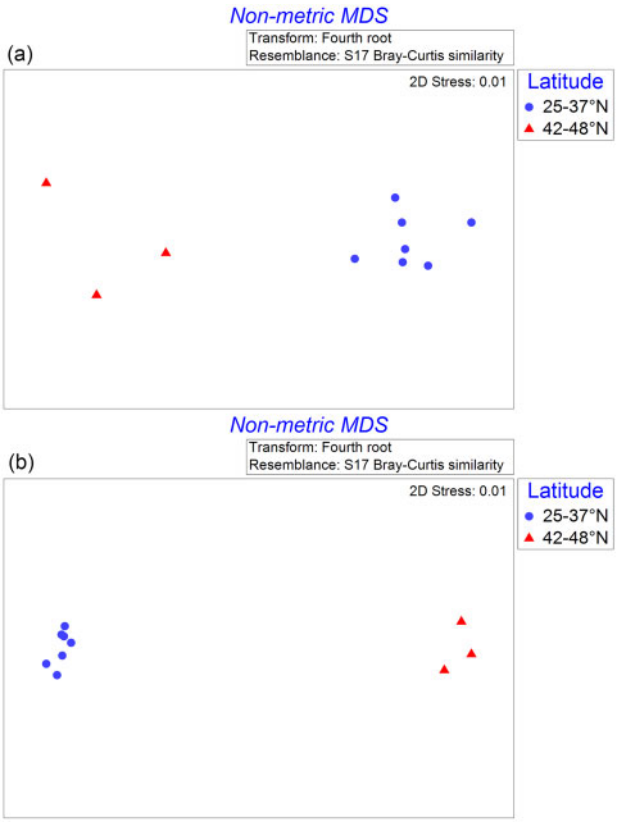

Figure 5. nMDS of the meso- and bathypelagic fish community, taking in count (a) density and (b) biomass.

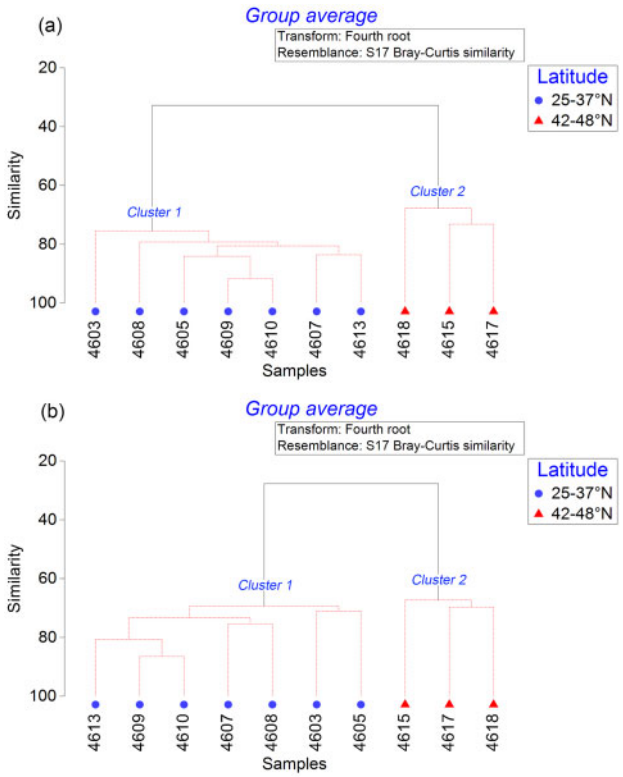

Figure 6. Dendrogram of station similarities (Bray–Curtis) based on (a) taxa density (fourth root transformed number/1000 m^3) and (b) biomass (fourth root transformed g wet weight/1000 m^3). Continuous blk lines denote significant group samples defined by the SIMPROF test (significance level of 1%).

the dominant taxon in meso- and bathypelagic ecosystems, both in the North Atlantic (Opdal *et al.*, 2008; Sutton *et al.*, 2010; Olivar *et al.*, 2017; Kenchington *et al.*, 2020) and oceans worldwide (Miya and Nemoto, 1987; Collins *et al.*, 2012; Davison *et al.*, 2015). The rank of the *Cyclothone* species changes with the latitudinal gradient, with the southern area dominated by *C. braueri* and the northern area by *C. microdon*, a species charteristic for the northern North Atlantic (Kenchington *et al.*, 2020). In the tropical and equatorial Atlantic, the occurrence and abundance of *Cyclothone parapallida* have been correlated with zones where AAIW occupies the mesopelagic layers, whereas *Cyclothone livida* increases in abundance when the AAIW disappears from the mesopelagic layers (Olivar *et al.*, 2017).

A crucial first step towards the effective and sustainable ecosystem management is understanding the distribution of marine biodiversity (Webb *et al.*, 2010). In this study, diversity (expressed as species richness) was lowest at the northern stations. There is no clear lower abundance (in terms of density) in the northern stations, but lower biomasses were recorded from 35°N and northwards. Sutton *et al.* (2010) also reported higher diversity (expressed as both species richness and Shannon index) in the southern Sargasso Sea, as well as higher abundance. In the area of the Charlie-Gibbs Frture Zone, Cook *et al.* (2013) found a decrease in diversity (expressed as Shannon index) from southeast to northwest. This corresponds with a similar gradient in SST and underlying water masses, suggesting that water masses can play an important role in the configuration of spatial assemblages of mesopelagic fish (Olivar *et al.*, 2017). In addition, the present eddies could be the mechanism that enhance diversity in the southeast area (Cook *et al.*, 2013), highlighting the importance of hydrographic structures in fish spatial distribution.

The southern stations were dominated by *C. braueri*, *C. microdon*, and *C. pseudopallida* in terms of density and by *E. pelecanoides* in terms of biomass. The density and biomass of northern stations were dominated by *C. microdon*, *C. braueri*, and *B. glaciale* (Supplementary Figure S3). Community structure in highly productive regions is in general charterized by a few largely dominant species (Andersen *et al.*, 1997). The higher fluorescence values in comparison with the southern stations reflect the higher productivity in the northern area. It is important to note that at the time of the cruise, the high densities of salps observed in the northern region point to a salp bloom in the area, which could be an explanation for lower densities and biomass of fish registered. This pattern of lower diversity in cooler and more productive stations and an increase in diversity in warmer conditions was also reported in the mesopelagic community of the Scotia Sea, Southern Ocean (Collins *et al.*, 2012). This suggests that the latitudinal diversity gradient described for pelagic species (i.e. species richness peaking around the tropic warm and oligotrophic waters and decreasing gradually towards the cold and productive polar waters) (Longhurst *et al.*, 1995; Reygondeau and Dunn, 2019), also applies for meso- and bathypelagic species. Saunders and Tarling (2018) found that Bergmann's rule, i.e. that body size increases with decreasing temperature and increasing latitude, can be applied to the majority of biomass-dominant myctophid species in the Southern Ocean. The transect of our study covered more latitudes and the temperature gradient was lower, but still

Table 2. Average similarity obtained with SIMPER analyses for eh cluster from fourth root density data, with indication of taxa that contributed for a 95% cut-off.

	Cluster 1	Cluster 2
Latitude	25–37° N	42–48° N
Average similarity	79.81	69.6
Cyclothone braueri	9.76	17.81
Cyclothone pseudopallida	6.35	11.88
Cyclothone microdon	6.13	25.6
Valenciennellus tripunctulatus	4.88	–
Argyropelecus hemigymnus	4.33	–
Sternoptyx spp.	3.74	–
Chauliodus danae	3.72	–
Lobianchia dofleini	3.57	–
Eurypharynx pelecanoides	3.39	–
Vinciguerria poweriae	3.38	–
Notolychnus valdiviae	3.22	–
Hygophum hygomii	3.17	–
Bolinichthys indicus	3.14	–
Argyropelecus uleatus	2.93	–
*Melamphaes*spp.	2.9	–
Bonapartia pedaliota	2.87	–
Lampanyctus ater	2.79	2.74
Serrivomer beanii	2.64	–
Photostomias guernei	2.6	–
Sigmops elongatum	2.48	–
Benthosema suborbitale	2.06	–
Notoscopelus resplendens	1.98	–
Lampanyctus cuprarius	1.93	–
Hygophum reinhardtii	1.88	–
Chauliodus sloani	1.87	–
Lampanyctus alatus	1.85	–
Diogenichthys atlanticus	1.74	–
Searsia koefoedi	1.6	–
Hygophum taaningi	1.3	–
Myctophum punctatum	1.22	–
Benthosema glaciale	–	18.4
Maurolicus muelleri	–	9.51
Xenodermichthys copei	–	7.75
Notoscopelus kroyeri	–	2.27

Clusters identified by the SIMPROF routine in PRIMER (see Figure 6a).

Table 3. Average similarity in percentage obtained with SIMPER analyses for eh cluster from fourth root biomass data, with indication of taxa that contributed for a 95% cut-off.

	Cluster 1	Cluster 2
Latitude	25–37° N	42–48° N
Average similarity	69.53	70.86
Eurypharynx pelecanoides	8.13	–
Cyclothone braueri	6.94	12.24
Chauliodus danae	5.93	–
Cyclothone microdon	5.58	22.09
Serrivomer beanii	5.16	–
Cyclothone pseudopallida	4.93	9.24
Photostomias guernei	4.46	–
Valenciennellus tripunctulatus	4.15	–
Lampanyctus ater	4.12	3.98
Bolinichthys indicus	3.94	–
Melamphaes spp.	3.92	–
Argyropelecus hemigymnus	3.82	–
Bonapartia pedaliota	3.73	–
Argyropelecus uleatus	3.69	–
Lobianchia dofleini	3.44	–
Sternoptyx spp.	3.43	–
Chauliodus sloani	3.37	–
Sigmops elongatus	3.17	–
Lampanyctus cuprarius	3.02	–
Hygophum hygomii	2.91	–
Lampanyctus alatus	2.42	–
Notoscopelus resplendens	2.38	–
Hygophum taaningi	1.35	–
Diretmus argenteus	1.26	–
Benthosema glaciale	–	15.4
Lampanyctus crocodilus	–	13.99
Maurolicus muelleri	–	11.06
Xenodermichthys copei	–	8.3

Clusters identified by the SIMPROF routine in PRIMER (see Figure 6b).

four species (Supplementary Figure S4) from three different families comply with Bergmann's rule.

Oceanography

The transect covers a range of different water masses and there is a clear distinction between the southern and northern part of the section, i.e. south and north of ~38°N. The upper layers, 0–200 and 300–700 m, in the southern part are charterized by warmer, saltier water, and lower oxygen concentrations compared to the northern part. This region is influenced by the Azores current that transports warmer and more saline Atlantic Water (i.e. NW) to the waters off Northwest Africa. The observed low chlorophyll concentration at the surface layer (0–200 m) south of 38°N confirms the known low productivity within the STG (Longhurst *et al.*, 1995). The higher chlorophyll concentration observed in the northern part, with a clear maximum at station 136 lies in a region with a wind-induced deep mixed layer during winter that exhibits large spring blooms (Sutton *et al.*, 2017). The observed weak vertical stratification with narrow ranged temperature and salinity values in this region is in contrast with the more stratified waters in the southern part that had much larger spans in temperature and salinity that also increased southward. The SST shows the upwelling effect close to the Northwest African continent, but the known upwelling effect on the production (e.g. Longhurst *et al.* 1995) is not observed in chlorophyll concentrations at the stations. This is most likely because the southern stations are too far away from the upwelling region.

The influence of the North Atlantic OMZ in the region is observed at 300–700 and 700–1200 m depth in the southern part of the section, particular south of 28°N (including fish station 4603). These concentrations are low enough to function as hypoxic conditions for several fish taxa (Vaquer-Sunyer and Duarte, 2008). The presence of the MOW is observed in the high salinity at 700–1200 m depth from station 126 (32°N) and northwards. MOW is also charterized by relatively high oxygen values and low nutrient concentrations, due to its origin in the oligotrophic Mediterranean Sea (Howe *et al.*, 1974).

Biogeography in relation to oceanography

The two distinct clusters found in this study are largely in agreement with the two ecoregions defined by Sutton *et al.* (2017) in the same area. The two northernmost stations of the northern cluster are located in the North Atlantic drift ecoregion while the third is in the Central North Atlantic ecoregion. Note that ecoregion boundaries must be

Table 4. DistLM marginal test results and model selection for density data.

Variable	SS (tre)	Pseudo-F	*p*	Proportion of the variation			
Marginal DistLm test							
Temperature at 300–700 m	**4 826.6**	**12.749**	**0.0078**	**0.64555**	–	–	–
Oxygen at 300–700 m	2 930.9	4.5131	0.056	0.392	–	–	–
Oxygen at 700–1 200 m	333.5	0.32682	0.7394	0.044605	–	–	–
Variable	**AICc**	**SS(tre)**	**Pseudo-F**	***p***	**Prop.**	**Cumul.**	**res.df**
SequentalDistLM test							
+Temperatute at 300–700 m	**57.166**	**4 826.6**	**12.749**	**0.0095**	**0.64555**	**0.64555**	**7**

Significant variables ($p < 0.05$) are highlighted in bold.

Table 5. DistLM marginal test results and model selection for biomass data.

Variable	SS(tre)	Pseudo-F	*p*	Proportion of the variation			
Marginal DistLm test							
Temperature at 300–700 m	**5 463.8**	**9.7044**	**0.0072**	**0.58095**	–	–	–
Oxygen at 300–700 m	3 348.9	3.8708	0.0558	0.35608	–	–	–
Oxygen at 700–1 200 m	796.13	0.64735	0.5264	0.08465	–	–	–
Variable	**AICc**	**SS(tre)**	**Pseudo-F**	***p***	**Prop.**	**Cumul.**	**res.df**
SequentalDistLM test							
+Temperatute at 300–700 m	**60.738**	**5 463.8**	**9.7044**	**0.008**	**0.58095**	**0.58095**	**7**

Significant variables ($p < 0.05$) are highlighted in bold.

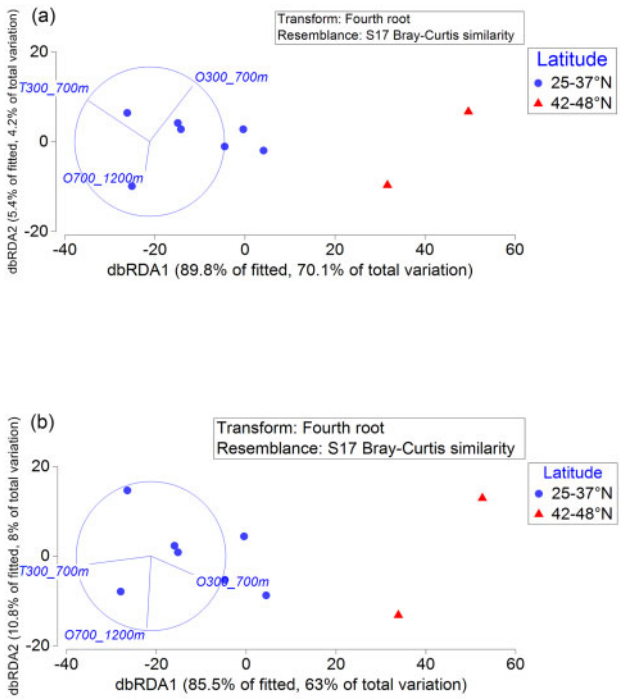

Figure 7. Distance-based redundancy analyses (dbRDA) to visualize the distance-based linear models (DISTLMs) in terms of (a) density and (b) biomass of the environmental variables in the study area. T300_700 m = average temperature from 300 to 700 m depth. O300_700m = average oxygen from 300 to 700 m. O700_1200m = average oxygen from 700 to 1200 m.

regarded as transitional zones and not as abrupt borders, and seasonal changes are not considered in the classification of Sutton *et al.* (2017). Altimeter data showed that the positions and number of branches of the North Atlantic Drift tend to shift from time to time as a consequence of long-lasting mesoscale eddies (Read *et al.*, 2010). The North Atlantic drift ecoregion is a transition between more boreal (e.g. *B. glaciale*, *Lampanyctus macdonaldi*, and *Protomyctophum arcticum*) and more subtropical species (e.g. *Paralepis brevirostris* and *Paralepis elongata*). All the stations belonging to the southern area correspond with the Central North Atlantic ecoregion (Sutton *et al.*, 2017). Along the northwest of Africa, high chlorophyll concentrations were expected due to upwelling effects. However, the observed chlorophyll concentrations were low in this area. This was most likely because the cruise transect was too far away from the African continent as discussed earlier.

In this work, the relationship between the fish assemblages and the temperature from 300 to 700 m depth was statistically significant. The latitudinal gradient in diversity is related to the temperature, which plays a key role in faunal distribution patterns (Sutton *et al.*, 2017). Each fish species has a thermal preference that optimizes physiological processes (Selleslagh and Amara, 2008). However, other environmental variables correlated with temperature at 300–700 m might be responsible for the changes in the fish community structure along the latitudinal gradient as well. Such correlated variables were not included in the models. If collinearity is ignored, it could result in misleading statistics without any significance and where dropping one covariate can make others significant or even change the sign of estimated parameters (Zuur *et al.*, 2010). For example, the fluorescence, which showed high collinearity with temperature at 300 to 700 m, is a proxy of primary production in surface waters, and primary production is a demonstrated driver of mesopelagic community biogeography (Sutton *et al.*, 2017).

Methodological aspects

The macrozooplankton trawl used in this study showed bias against capturing large fish and the lower size range of some species. For example, small species such as *C. braueri*, *H. hygomii*, or *N. valdiviae* differed only little from the maximum sizes reported in the literature, respectively, 38, 68, and 25 mm (Sutton *et al.*

2020), whereas larger species showed a bias towards the lower end of their size range, e.g. *Chauliodus sloani* (350 mm), *L. crocodilus* (172 mm), or *Sigmops elongatus* (275 mm) (Sutton *et al.*, 2020). The reasons of that bias could be avoidance of the large and fast swimming fish when trawling at low speeds (1 ms^{-1}; Gartner *et al.*, 1989; Kaartvedt *et al.*, 2012) and the relatively small mouth area of the net (~35 m^2).

Few individuals in the lower size range of *Cyclothone* spp. were caught with the 3 × 3 light-opening meshes, which agrees with previous studies (Gartner *et al.*, 1989; Olivar *et al.*, 2017). Gartner *et al.* (1989) showed that midwater trawls with mesh size of >2 mm underestimate the lower size range (fish smaller than 30-mm SL). The fact that Olivar *et al.* (2017) reported significantly higher sampling efficiency with plankton nets than with a midwater trawl with graded-mesh from 30 mm in the trawl opening to 4 mm in the cod-end could be explained by the larger meshes at the front of that trawl. The gear used in this study had the same mesh size throughout the trawl and therefore the selectivity of the trawl was constant.

In conclusion, the structure of fish assemblages in the Northeastern Atlantic changes along the latitudinal gradient. Fish community in the southern area was more diverse than in the northern region and temperature seems to be an important factor in species distribution. Although many species are present in both areas, abundance, rank and, though on a small scale, sizes changed. Overall, this study improves our understanding on the variation in deep-pelagic ecosystems on a large spatial scale and given its value in the provision of ecosystem services, this information is essential to the ecosystem management approach and marine spatial planning.

Supplementary data

Supplementary material is available at the *ICESJMS* online version of the manuscript.

Data availability

Data are available on request.

Acknowledgements

We are grateful to the captain and the crew on board the *R.V.* "Kronprins Haakon", and to all the colleagues who participated in the cruise. We knowledge the editor and the two anonymous referees for their constructive comments on the manuscript.

Funding

This research has been founded by HARMES (Research Council of Norway project number 280546) and MEESO (EU H2020 research and innovation programme, Grant Agreement No. 817669).

References

Andersen, V., Sardou, J., and Gasser, B. 1997. Mroplankton and micronekton in the northeast tropical Atlantic: abundance, community composition and vertical distribution in relation to different trophic environments. Deep Sea Research Part I: Oceanographic Research Papers, 44: 193–222.

Anderson, M. J., Gorley, R. N., and Clarke, R. K. 2008. Permanova+ for Primer: Guide to Software and Statistical Methods. Primer-E Ltd, Plymouth, UK. 214 pp.

Ariza, A., Landeira, J. M., Escánez, A., Wienerroither, R., Aguilar de Soto, N., Røstad, A., Kaartvedt, S. *et al.* 2016. Vertical distribution, composition and migratory patterns of oustic scattering layers in the Canary Islands. Journal of Marine Systems, 157: 82–91.

Backus, R. H., Craddock, J. E., Haedrich, R. L., and Robison, B. H. 1977. Atlantic mesopelagic zoogeography. *In* Fishes of the Western North Atlantic. Part 7. Vol 1, pp. 266–287. Ed. by R.H. Gibbs Jr. Memoir Sears Foundation of Marine Research.

Badcock, J. 1984. Gonostomatidae. *In* Fishes of the North-Eastern Atlantic and the Mediterranean, pp. 284–301. Ed. by P. J. P. Whitehead, M. L. Bauchot, J. C. Hureau, J. Nielsen, and E. Tortonese. UNESCO, Paris.

Bashmhnikov, I., Nascimento, Â., Neves, F., Menezes, T., and Koldunov, N. V. 2015. Distribution of intermediate water masses in the subtropical northeast Atlantic. Ocean Science, 11: 803–827.

Carpenter, K. E., and De Angelis, N. 2016. The living marine resources of the Eastern Central Atlantic. FAO, Rome.

Carredo, L. I., Pardo, P. C., Flecha, S., and Pérez, F. F. 2016. On the Mediterranean water composition. Journal of Physical Oceanography, 46: 1339–1358.

Clarke, K. R., and Gorley, R. N. 2015. PRIMER v7: User Manual/Tutorial. PRIMER-E Ltd, Plymouth. 296 pp.

Clarke, K. R., Gorley, R. N., Somerfield, P. J., and Warwick, R. M. 2014. Change in Marine Communities: An Approh to Statistical Analysis and Interpretation. Primer-E Ltd, Plymouth. 256 pp.

Collins, M. A., Stowasser, G., Fielding, S., Shreeve, R., Xavier, J. C., Venables, H. J., Enderlein, P. *et al.* 2012. Latitudinal and bathymetric patterns in the distribution and abundance of mesopelagic fish in the Scotia Sea. Deep Sea Research Part II: Topical Studies in Oceanography, 59–60: 189–198.

Cook, A. B., Sutton, T. T., Galbraith, J. K., and Vecchione, M. 2013. Deep-pelagic (0–3000m) fish assemblage structure over the Mid-Atlantic Ridge in the area of the Charlie-Gibbs Frture Zone. Deep Sea Research Part II: Topical Studies in Oceanography, 98: 279–291.

Davison, P. C., Checkley, D. M. Jr, Koslow, J. A., and Barlow, J. 2013. Carbon export mediated by mesopelagic fishes in the northeast Pific Ocean. Progress in Oceanography, 116: 14–30.

Davison, P. C., Koslow, J. A., and Kloser, R. J. 2015. oustic biomass estimation of mesopelagic fish: bkscattering from individuals, populations, and communities. ICES Journal of Marine Science, 72: 1413–1424.

Donlon, C. J., Martin, M., Stark, J., Roberts-Jones, J., Fiedler, E., and Wimmer, W. 2012. The Operational Sea Surfe Temperature and Sea Ice Analysis (OSTIA) system. Remote Sensing of Environment, 116: 140–158.

Drazen, J. C., and Sutton, T. T. 2017. Dining in the deep: the feeding ecology of deep-sea fishes. Annual Review of Marine Science, 9: 337–366.

Fricke, R., Eschmeyer, W. N., and van der Laan, R. 2020. Eschmeyer's Catalog of Fishes: Genera, Species, References. http://researcharchive.calademy.org/research/ichthyology/catalog/fishcatmain.asp (last cessed 12 June 2020).

García-Seoane, E., Vieira, R. P., Moreno, A., Caldeira, R. M. A., Azevedo, C. C., Gaudêncio, M. J., and dos Santos, A. 2020. Distribution and diversity of mesopelagic fauna on seamounts of the Madeira-Tore complex (Northeastern Atlantic). Regional Studies in Marine Science, 39: 101434.

Gartner, J. V. Jr, Conley, W. J., and Hopkins, T. L. 1989. Escapement by fishes from midwater trawls: a case study using lanternfishes (Pisces: Myctophidae). Fishery Bulletin, 87: 213–222.

Gibbs, R. H. Jr. 1984. Astronesthidae, Chauliodontidae, Stomiidae, Melanostomiidae, Malosteidae, Idianthidae. *In* Fishes of the North-Eastern Atlantic and the Mediterranean, pp. 325–372. Ed. by P. J. P. Whitehead, M. L. Bauchot, J. C. Hureau, J. Nielsen, and E. Tortonese. UNESCO, Paris.

Gjøsæter, J., and Kawaguchi, K. 1980. A review of the world resources of mesopelagic fish. FAO Fish Technical Papers, 193: 1–153.

Heino, M., Porteiro, F. M., Sutton, T. T., Falkenhaug, T., Godø, O. R., and Piatkowski, U. 2011. Catchability of pelagic trawls for sampling deep-living nekton in the mid-North Atlantic. ICES Journal of Marine Science, 68: 377–389.

Howe, M. R., Abdullah, M. I., and Deetae, S. 1974. An interpretation of the double TS maxima in the Mediterranean outflow using chemical trers. Journal of Marine Research, 32: 377–386.

Hulley, P. A. 1984. Myctophidae. *In* Fishes of the North-Eastern Atlantic and the Mediterranean, pp. 429–483. Ed. by P. J. P. Whitehead, M. L. Bauchot, J. -C. Hureau, J. Nielsen, and E. Tortonese. UNESCO, Paris.

Hulley, P. A., and Lutjeharms, J. R. 1989. Lanternfishes of the southern Benguela region. Part 3. The pseudoceanic-oceanic interfe. Annals of the South African Museum, 98: 1–10.

Irigoien, X., Klevjer, T. A., Røstad, A., Martinez, U., Boyra, G., uña, J. L., Bode, A. *et al.* 2014. Large mesopelagic fishes biomass and trophic efficiency in the open ocean. Nature Communications, 5: 1–10.

Kaartvedt, S., Staby, A., and Aksnes, D. L. 2012. Efficient trawl avoidance by mesopelagic fishes causes large underestimation of their biomass. Marine Ecology Progress Series, 456: 1–6.

Kenchington, T. J., Themelis, D. E., DeVaney, S. C., and Kenchington, E. L. 2020. The meso- and bathypelagic fishes in a large submarine canyon: assemblage structure of the principal species in the Gully Marine Protected Area. Frontiers in Marine Science, 7: 181.

Krafft, B. A., Melle, W., Knutsen, T., Bagøien, E., Broms, C., Ellertsen, B., and Siegel, V. 2010. Distribution and demography of Antarctic krill in the Southeast Atlantic sector of the Southern Ocean during the austral summer 2008. Polar Biology, 33: 957–968.

Legendre, P., and Anderson, M. J. 1999. Distance-based redundancy analysis: testing multispecies responses in multiftorial ecological experiments. Ecological Monographs, 69: 1–24.

Longhurst, A., Sathyendranath, S., Platt, T., and Caverhill, C. 1995. An estimate of global primary production in the ocean from satellite radiometer data. Journal of Plankton Research, 17: 1245–1271.

Machín, F., and Pelegrí, J. L. 2009. Northward penetration of Antarctic Intermediate Water off Northwest Africa. Journal of Physical Oceanography, 39: 512–535.

McArdle, B. H., and Anderson, M. J. 2001. Fitting multivariate models to community data: a comment on distance based redundancy analysis. Ecology, 82: 290–297.

Mengerink, K. J., Van Dover, C. L., Ardron, J., Baker, M., Escobar-Briones, E., Gjerde, K., Koslow, J. A. *et al.* 2014. A call for deep-ocean stewardship. Science, 344: 696–698.

Miya, M., and Nemoto, T. 1987. Reproduction, growth and vertical distribution of the meso- and bathypelagic fish *Cyclothone atraria* (Pisces: Gonostomatidae) in Sagami Bay, Central Japan. Deep Sea Research Part A. Oceanographic Research Papers, 34: 1565–1577.

Mjanger, H., Svendsen, B. V., H, S., Å, F., S, M., and A, S. 2017. Håndbok for prøvetaking av fisk og krepsdyr. Versjon 3.16. Havforskningsinstituttets kvalitetssystem, 194 pp (in Norwegian).

O'Connor, B. M., Fine, R. A., and Olson, D. B. 2005. A global comparison of subtropical underwater formation rates. Deep Sea Research Part I: Oceanographic Research Papers, 52: 1569–1590.

Olivar, M. P., Hulley, P. A., Castellón, A., Emelianov, M., López, C., Tuset, V. M., Contreras, T. *et al.* 2017. Mesopelagic fishes ross the tropical and equatorial Atlantic: biogeographical and vertical patterns. Progress in Oceanography, 151: 116–137.

Opdal, A. F., Godø, O. R., Bergstad, O. A., and Fiksen, Ø. 2008. Distribution, identity, and possible processes sustaining meso- and bathypelagic scattering layers on the northern Mid-Atlantic Ridge. Deep Sea Research Part II: Topical Studies in Oceanography, 55: 45–58.

Pollard, R. T., Griffttths, M. J., Cunningham, S. A., Read, J. F., Pérez, F. F., and Ríos, A. F. 1996. Vivaldi 1991-A study of the formation, circulation and ventilation of Eastern North Atlantic Central Water. Progress in Oceanography, 37: 167–192.

Porteiro, F. M., and Sutton, T. 2007. Midwater fish assemblages and seamounts. *In* Seamounts: Ecology, Fisheries, and Conservation, pp. 101–116. Ed. by T. J. Pitcher, T. Morato, P. J. B. Hart, M. R. Clark, N. Haggan, and R. S. Santos. Blackwell Publishing, Oxford, UK.

Proud, R., Handegard, N. O., Kloser, R. J., Cox, M. J., and Brierley, A. S. 2019. From siphonophores to deep scattering layers: uncertainty ranges for the estimation of global mesopelagic fish biomass. ICES Journal of Marine Science, 76: 718–733.

R Development Core Team. 2019. R: A Language and Environment for Statistical Computing. R Foundation for statistical computing, Viena, Austria. URL:http://www.R-project.org

Read, J. F., Pollard, R. T., Miller, P. I., and Dale, A. C. 2010. Circulation and variability of the North Atlantic Current in the vicinity of the Mid-Atlantic Ridge. Deep Sea Research Part I: Oceanographic Research Papers, 57: 307–318.

Reygondeau, G., and Dunn, D. 2019. Pelagic biogeography. *In* Encyclopedia of Ocean Sciences, pp. 588–598. Ed. by J. K. Cochran, H. J. Bokuniewicz, and P. L. Yager. Academic Press.

Ríos, A. F., Pérez, F. F., and Fraga, F. 1992. Water masses in the upper and middle North Atlantic Ocean east of the Azores. Deep Sea Research Part A. Oceanographic Research Papers, 39: 645–658.

Robinson, C., Steinberg, D. K., Anderson, T. R., Arístegui, J., Carlson, C. A., Frost, J. R., Ghiglione, J.-F., *et al.* 2010. Mesopelagic zone ecology and biogeochemistry—a synthesis. Deep Sea Research Part II: Topical Studies in Oceanography, 57: 1504–1518.

Saunders, R. A., and Tarling, G. A. 2018. Southern Ocean mesopelagic fish comply with Bergmann's rule. The American Naturalist, 191: 343–351.

Selleslagh, J., and Amara, R. 2008. Environmental ftors structuring fish composition and assemblages in a small mrotidal estuary (eastern English Channel). Estuarine, Coastal and Shelf Science, 79: 507–517.

Stramma, L., and England, M. 1999. On the water masses and mean circulation of the South Atlantic Ocean. Journal of Geophysical Research: Oceans, 104: 20863–20883.

Sutton, T. T. 2013. Vertical ecology of the pelagic ocean: classical patterns and new perspectives. Journal of Fish Biology, 83: 1508–1527.

Sutton, T. T., Clark, M. R., Dunn, D. C., Halpin, P. N., Rogers, A. D., Guinotte, J., Bograd, S. J. *et al.* 2017. A global biogeographic classification of the mesopelagic zone. Deep Sea Research Part I: Oceanographic Research Papers, 126: 85–102.

Sutton, T. T., Hulley, P. A., Wienerroither, R., Zaera-Perez, D., and Paxton, J. R. 2020. Identification guide to the mesopelagic fishes of the Central and South East Atlantic Ocean, FAO, Rome.

Sutton, T. T., Porteiro, F. M., Heino, M., Byrkjedal, I., Langhelle, G., Anderson, C. I. H., Horne, J. *et al.* 2008. Vertical structure, biomass and topographic association of deep-pelagic fishes in relation to a mid-ocean ridge system. Deep Sea Research Part II: Topical Studies in Oceanography, 55: 161–184.

Sutton, T. T., Wiebe, P. H., Madin, L., and Bucklin, A. 2010. Diversity and community structure of pelagic fishes to 5000m depth in the Sargasso Sea. Deep Sea Research Part II: Topical Studies in Oceanography, 57: 2220–2233.

Tenore, K. R., Alonso-Noval, M., Alvarez-Ossorio, M., Atkinson, L. P., Cabanas, J. M., Cal, R. M., Campos, H. J., *et al.* 1995. Fisheries and oceanography off Galicia, NW Spain: Mesoscale spatial and temporal changes in physical processes and resultant patterns of biological productivity. Journal of Geophysical Research: Oceans, 100: 10943–10966.

Thurber, A. R., Sweetman, A. K., Narayanaswamy, B. E., Jones, D. O. B., Ingels, J., and Hansman, R. L. 2014. Ecosystem function and services provided by the deep sea. Biogeosciences, 11: 3941–3963.

Valdés, L., and Déniz-Gonzalez, I. 2015. Oceanographic and biological features in the Canary Current Large Marine Ecosystem. IOC-UNESCO, Paris.

van der Laan, R., Fricke, R., and Eschmeyer, W. N. 2020. Eschmeyer's Catalog of Fishes: Classification. http://www.calademy.org/scientists/catalog-of-fishes-classification (last cessed 12 June 2020).

Vaquer-Sunyer, R., and Duarte, C. M. 2008. Thresholds of hypoxia for marine biodiversity. Proceedings of the National ademy of Sciences of the United States of America, 105: 15452–15457.

Webb, T. J., Vanden Berghe, E., and O'Dor, R. 2010. Biodiversity's big wet wecret: the global distribution of marine biological records reveals chronic under-exploration of the deep pelagic ocean. PLoS One, 5: e10223.

Whitehead, P. J. P., Bauchot, M. L., Hureau, J. C., Nielsen, J., and Tortonese, E. 1984–1986. Fishes of the North-Eastern Atlantic and the Mediterranean. UNESCO, Paris.

Wienerroither, R., Uiblein, F., Bordes, F., and Moreno, T. 2009. Composition, distribution, and diversity of pelagic fishes around the Canary Islands, Eastern Central Atlantic. Marine Biology Research, 5: 328–344.

Zuur, A. F., Ieno, E. N., and Elphick, C. S. 2010. A protocol for data exploration to avoid common statistical problems. Methods in Ecology and Evolution, 1: 3–14.

Handling editor: Roland Proud